

Theory of Unitary Spin Rotation and Spin State Tomography for a Single Electron and Two Electrons

T. Takagahara

*Department of Electronics and Information Science,
Kyoto Institute of Technology, Matsugasaki, Kyoto 606-8585
CREST, Japan Science and Technology Agency,
4-1-8 Honcho, Kawaguchi, Saitama 332-0012,
Japan*

1. Introduction

Coherent control of quantum states is a critical step toward many novel technological applications ranging from manipulation of quantum bits (qubits) in quantum logic gates to controlling the spin degrees of freedom of electrons [1–13]. A qubit with a longer coherence time is desirable for the application to the quantum information processing. Electron spins in semiconductor nanostructures are considered as one of the most promising candidates of the building blocks for quantum information processing due to their robustness against decoherence effects [14–18]. A quantum media converter between a photon qubit and an electron spin qubit was proposed for the use in quantum repeaters [19–22]. Quantum information can take several different forms and it is preferable to be able to convert among different forms. One form is the photon polarization and another is the electron spin polarization. Photons are the most convenient medium for sharing quantum information between distant locations. Electrons are the most efficient medium for manipulating the quantum information by electrical and optical means. The fundamental operations are the initialization, unitary rotation and measurement of a qubit. The initialization of a single electron spin was demonstrated by the efficient optical method [23–25]. Also, the coherent rotation of a single electron spin has been realized by the microwave ESR (Electron Spin Resonance) method [26] and by the optical STIRAP (STImulated Raman Adiabatic Passage) method with coherence times up to several μs [27–33] in III-V semiconductor nanostructures and up to several tens of ms in the localized electron systems in IV elemental semiconductors [34–36]. The optical STIRAP method is advantageous because of its ultrafast operation. However, the precise control of the spin rotation without leaving behind any population in the intermediate excited states has not yet been realized. It is also important to achieve the unitary spin rotation of two electrons, because the singlet-triplet subspace of two electrons was utilized as a qubit space and the electrical manipulation of the qubit was realized [16]. At the same time, it is absolutely necessary to confirm the quantum state of the electron after the spin state manipulation or the quantum state transfer from a photon, namely, to examine whether the electron spin is prepared in the desired state or not. This

Source: *Advances in Lasers and Electro Optics*, Book edited by: Nelson Costa and Adolfo Cartaxo, ISBN 978-953-307-088-9, pp. 838, April 2010, INTECH, Croatia, downloaded from SCIYO.COM

requires the full state tomography, namely the measurement of the density matrix of the electron. This state tomography is also important to estimate the fidelity of relevant quantum operations.

Thus it is a challenging task to establish the precise spin rotation and the spin state tomography for both cases of a single electron and two electrons. We review the general aspects of the unitary spin rotation of a single electron by the STIRAP method and develop the scheme to rotate the pseudo-spin formed by the singlet state and the triplet states of two electrons based on the optical STIRAP process, discussing the optimal conditions for the precise control. Also we propose and analyze optical methods to achieve the electron spin state tomography based on the Faraday/Kerr rotation, referring to the recent experiments [37, 38].

2. Optical STIRAP method for spin rotation of a single electron

As mentioned in the Introduction, the spin rotation of a single electron is a crucial ingredient in the quantum information processing. It is desirable to accomplish the spin rotation along an arbitrary direction for an arbitrary rotation angle in a single-shot process. So far, the spin rotation of a single electron was demonstrated by optical and electrical means in the proof-of-principle experiments. With respect to the required time for the spin rotation, the optical method based on the STIRAP (stimulated Raman adiabatic passage) process is preferable because of its ultrafast response. But the precise control of the spin rotation is yet to be pursued. Here several characteristics of this STIRAP process will be investigated.

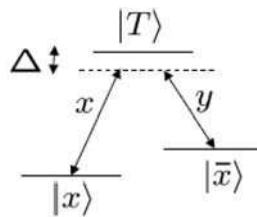


Fig. 1. Schematic energy level structure for the STIRAP process. Allowed optical transitions are depicted by x and y , which represent the mutually orthogonal polarizations. Δ denotes the off-resonance energy of the excitation lights relative to the transition energies. The Raman condition for the excitation lights is imposed.

In order to carry out the STIRAP process, a Λ -type transition is necessary, as depicted in Fig. 1. The lowest two levels denoted by $|x\rangle$ and $|\bar{x}\rangle$ are the ground doublet states with close energies, e.g., the spin up and spin down states of a single electron or the ground and excited vibrational states of a single molecule. A pseudospin is composed of these doublet states and can be rotated by optical transitions via the intermediate excited state denoted by $|T\rangle$. The important point is that the selection rules of the left and right optical transitions are orthogonal to each other, which are depicted typically as x and y in Fig. 1. The doublet states are not directly connected optically. Then the relevant Hamiltonian is written as

$$H = H_0 + V, \quad (1)$$

$$H_0 = E_x|x\rangle\langle x| + E_{\bar{x}}|\bar{x}\rangle\langle \bar{x}| + E_T|T\rangle\langle T|, \tag{2}$$

$$V = -\hbar\Omega_x(t)[e^{-i\omega_x t}|T\rangle\langle x| + e^{i\omega_x t}|x\rangle\langle T|] \\ -\hbar\Omega_y(t)[e^{-i\omega_y t-i\delta}|T\rangle\langle \bar{x}| + e^{i\omega_y t+i\delta}|\bar{x}\rangle\langle T|], \tag{3}$$

where H_0 represents the unperturbed part, V the optical transitions, Ω_x and Ω_y the Rabi frequencies, δ the relative phase shift of the y -polarized light and the energy E_x is put as $E_x = 0$ for the origin of energy. Then the time evolution proceeds as follows:

$$i\hbar\dot{\psi} = H\psi, \quad \psi = c_x|x\rangle + c_{\bar{x}}|\bar{x}\rangle + c_T|T\rangle, \tag{4}$$

$$\frac{d}{dt} \begin{pmatrix} c_x \\ c_{\bar{x}} \\ c_T \end{pmatrix} = \begin{pmatrix} i\Omega_x(t)e^{i\omega_x t}c_T \\ -i\frac{E_{\bar{x}}}{\hbar}c_{\bar{x}} + i\Omega_y(t)e^{i\omega_y t+i\delta}c_T \\ -i\frac{E_T}{\hbar}c_T + i\Omega_x(t)e^{-i\omega_x t}c_x + i\Omega_y(t)e^{-i\omega_y t-i\delta}c_{\bar{x}} \end{pmatrix}. \tag{5}$$

In order to single out the rapidly oscillating part, we put as

$$c_{\bar{x}}(t) = e^{-i\frac{E_{\bar{x}}}{\hbar}t}\tilde{c}_{\bar{x}}(t), \quad c_T(t) = e^{-i\frac{E_T}{\hbar}t}\tilde{c}_T(t), \tag{6}$$

obtaining

$$\frac{d}{dt} \begin{pmatrix} c_x \\ \tilde{c}_{\bar{x}} \\ \tilde{c}_T \end{pmatrix} = \begin{pmatrix} i\Omega_x(t)e^{i(\omega_x - \frac{E_T}{\hbar})t}\tilde{c}_T \\ i\Omega_y(t)e^{i(\omega_y - \frac{E_T}{\hbar} + \frac{E_{\bar{x}}}{\hbar})t+i\delta}\tilde{c}_T \\ i\Omega_x(t)e^{-i(\omega_x - \frac{E_T}{\hbar})t}c_x + i\Omega_y(t)e^{-i(\omega_y - \frac{E_T}{\hbar} + \frac{E_{\bar{x}}}{\hbar})t-i\delta}\tilde{c}_{\bar{x}} \end{pmatrix}. \tag{7}$$

Now we postulate the Raman condition for the x and y polarized lights:

$$\frac{E_T}{\hbar} - \omega_x = \frac{E_T}{\hbar} - \frac{E_{\bar{x}}}{\hbar} - \omega_y = \Delta \tag{8}$$

and also assume the same pulse shape for the x - and y -polarized lights with arbitrary relative intensity ratio determined by θ :

$$\Omega_x(t) = \Omega_0(t) \cos \theta, \quad \Omega_y(t) = \Omega_0(t) \sin \theta. \tag{9}$$

Introducing the bright and dark state amplitudes defined by

$$\begin{pmatrix} c_B \\ c_D \end{pmatrix} = \begin{pmatrix} \cos \theta & e^{-i\delta} \sin \theta \\ -e^{i\delta} \sin \theta & \cos \theta \end{pmatrix} \begin{pmatrix} c_x \\ \tilde{c}_{\bar{x}} \end{pmatrix} = U \begin{pmatrix} c_x \\ \tilde{c}_{\bar{x}} \end{pmatrix}, \tag{10}$$

we can simplify the equations of motion as

$$\frac{d}{dt} \begin{pmatrix} c_B \\ \tilde{c}_T \end{pmatrix} = \begin{pmatrix} i\Omega_0(t)e^{-i\Delta t} \tilde{c}_T \\ i\Omega_0(t)e^{i\Delta t} c_B \end{pmatrix}, \quad \frac{d}{dt}c_D = 0. \tag{11}$$

Thus the dark state does not change. The amplitudes of the bright state and the $|T\rangle$ state satisfy the following equations:

$$\frac{d^2}{dt^2} c_B = \left(\frac{\dot{\Omega}_0(t)}{\Omega_0(t)} - i\Delta \right) \frac{d}{dt} c_B - \Omega_0^2(t) c_B, \tag{12}$$

$$\frac{d^2}{dt^2} \tilde{c}_T = \left(\frac{\dot{\Omega}_0(t)}{\Omega_0(t)} + i\Delta \right) \frac{d}{dt} \tilde{c}_T - \Omega_0^2(t) \tilde{c}_T. \tag{13}$$

To develop the analytical solutions of these equations [39, 40], we assume a sech pulse envelope:

$$\Omega_0(t) = \Omega \operatorname{sech}(\sigma t). \tag{14}$$

Introducing a dimensionless time variable by

$$\zeta = \frac{1}{2}(1 + \tanh(\sigma t)), \tag{15}$$

we have

$$\zeta(1 - \zeta) \frac{d^2}{d\zeta^2} c_B + \left(\frac{1}{2} \left(1 + i \frac{\Delta}{\sigma} \right) - \zeta \right) \frac{d}{d\zeta} c_B + \frac{\Omega^2}{\sigma^2} c_B = 0, \tag{16}$$

$$\zeta(1 - \zeta) \frac{d^2}{d\zeta^2} \tilde{c}_T + \left(\frac{1}{2} \left(1 - i \frac{\Delta}{\sigma} \right) - \zeta \right) \frac{d}{d\zeta} \tilde{c}_T + \frac{\Omega^2}{\sigma^2} \tilde{c}_T = 0. \tag{17}$$

This is a hypergeometric differential equation. General solutions are given by

$$\begin{pmatrix} c_B(t) \\ \tilde{c}_T(t) \end{pmatrix} = \begin{pmatrix} F(\alpha, -\alpha, \gamma | \zeta) & e^{i\Delta t} \frac{i\alpha}{\gamma} \zeta^{\gamma^*} F(\alpha + \gamma^*, -\alpha + \gamma^*, 1 + \gamma^* | \zeta) \\ e^{-i\Delta t} \frac{i\alpha}{\gamma} \zeta^{\gamma} F(\alpha + \gamma, -\alpha + \gamma, 1 + \gamma | \zeta) & F(\alpha, -\alpha, \gamma | \zeta) \end{pmatrix} \times \begin{pmatrix} c_B(-\infty) \\ \tilde{c}_T(-\infty) \end{pmatrix} \tag{18}$$

$$\text{with } \alpha = \frac{\Omega}{\sigma}, \beta = -\frac{\Omega}{\sigma}, \gamma = \frac{1}{2} \left(1 + i \frac{\Delta}{\sigma} \right), \tag{19}$$

where $F(\alpha, \beta, \gamma | \zeta)$ is the hypergeometric function. In the rotation of the pseudospin, we start with the initial state in which

$$c_B(-\infty) = \text{finite}, c_D(-\infty) = \text{finite}, \tilde{c}_T(-\infty) = 0 \tag{20}$$

and after the pulse we prefer to have

$$\tilde{c}_T(\infty) = 0 \tag{21}$$

in order to leave no excitation in the intermediate excited state $|T\rangle$. To satisfy this condition, we should have

$$\frac{\alpha}{\gamma} F(\alpha + \gamma, -\alpha + \gamma, 1 + \gamma|1) = 0 \tag{22}$$

because the asymptotic behavior ($t \rightarrow \infty$) is given by putting as $\zeta = 1$. Using the formula [41]

$$F(a, b, c|1) = \frac{\Gamma(c)\Gamma(c-a-b)}{\Gamma(c-a)\Gamma(c-b)} \tag{23}$$

which is valid under the condition that $\text{Re}(c-a-b) > 0$ and $c \neq 0, -1, -2, \dots$, we have

$$\frac{\alpha}{\gamma} F(\alpha + \gamma, -\alpha + \gamma, 1 + \gamma|1) = \frac{\alpha \Gamma(1 + \gamma)\Gamma(1 - \gamma)}{\gamma \Gamma(1 - \alpha)\Gamma(1 + \alpha)}. \tag{24}$$

Further, using the formulas

$$x\Gamma(x) = \Gamma(x + 1), \quad \Gamma(x)\Gamma(1 - x) = \frac{\pi}{\sin \pi x}, \tag{25}$$

we obtain

$$\frac{\alpha \Gamma(1 + \gamma)\Gamma(1 - \gamma)}{\gamma \Gamma(1 - \alpha)\Gamma(1 + \alpha)} = \frac{\alpha \gamma \Gamma(\gamma)\Gamma(1 - \gamma)}{\gamma \Gamma(1 - \alpha)\alpha\Gamma(\alpha)} = \frac{\sin \pi \alpha}{\sin \pi \gamma}. \tag{26}$$

Putting in the expression of γ , we finally have

$$\frac{\alpha}{\gamma} F(\alpha + \gamma, -\alpha + \gamma, 1 + \gamma|1) = \text{sech} \left(\frac{\pi \Delta}{2\sigma} \right) \sin \pi \alpha. \tag{27}$$

This quantity vanishes only when $\alpha = 1, 2, \dots$. This condition is nothing but the condition that the pulse area is $2\pi, 4\pi, \dots$. This is quite reasonable because the Bloch vector rotates and returns to the initial state for the pulse area of integer times 2π .

Furthermore, under this condition, the amplitude of the bright state receives after a pulse an additional factor given by

$$F(\alpha, -\alpha, \gamma|1) = -\frac{\gamma^*}{\gamma}, \frac{\gamma^*(\gamma^* + 1)}{\gamma(\gamma + 1)}, -\frac{\gamma^*(\gamma^* + 1)(\gamma^* + 2)}{\gamma(\gamma + 1)(\gamma + 2)} \dots, \tag{28}$$

where the expressions on the right hand side correspond to $\alpha = 1, 2, 3, \dots$, respectively and their absolute magnitude is obviously unity and thus they can be put as

$$F(\alpha, -\alpha, \gamma|1) = e^{-i\phi}. \tag{29}$$

This phase ϕ determines the rotation angle of the pseudospin, as will be shown shortly. Now the effect of the pulse can be summarized as

$$\begin{pmatrix} c_B(\infty) \\ c_D(\infty) \end{pmatrix} = \begin{pmatrix} e^{-i\phi} & 0 \\ 0 & 1 \end{pmatrix} \begin{pmatrix} c_B(-\infty) \\ c_D(-\infty) \end{pmatrix} . \tag{30}$$

This relation can be rewritten in terms of $(c_x, \tilde{c}_{\bar{x}})$ amplitudes:

$$\begin{pmatrix} c_x(\infty) \\ \tilde{c}_{\bar{x}}(\infty) \end{pmatrix} = U^\dagger \begin{pmatrix} e^{-i\phi} & 0 \\ 0 & 1 \end{pmatrix} U \begin{pmatrix} c_x(-\infty) \\ \tilde{c}_{\bar{x}}(-\infty) \end{pmatrix} , \tag{31}$$

where the operation of the pulse is calculated as

$$\begin{aligned} U^\dagger \begin{pmatrix} e^{-i\phi} & 0 \\ 0 & 1 \end{pmatrix} U &= e^{-i\phi/2} \left[\cos \frac{\phi}{2} \mathbf{1} - i \sin \frac{\phi}{2} (\vec{n} \cdot \vec{\sigma}) \right] = e^{-i\phi/2} \exp \left[-i \frac{\phi}{2} \vec{n} \cdot \vec{\sigma} \right] \\ &= e^{-i\phi/2} \exp \left[-i\phi \vec{n} \cdot \vec{S} \right] \end{aligned} \tag{32}$$

$$\text{with } \vec{n} = (\sin 2\theta \cos \delta, \sin 2\theta \sin \delta, \cos 2\theta) , \quad \tan \theta = \frac{\Omega_y}{\Omega_x} . \tag{33}$$

This relation indicates that the pseudospin vector composed of $|x\rangle$ and $|\bar{x}\rangle$ states is rotated by an angle ϕ around the direction vector \vec{n} . The rotation angle ϕ can be tuned by the off-resonance energy Δ in Eq. (8), whereas the direction vector \vec{n} can be adjusted by the intensity ratio and the relative phase shift between the orthogonally polarized lights with the same temporal envelope.

In order to estimate the fidelity of this spin rotation, we prepare an arbitrary initial state, follow the time evolution to obtain the asymptotic state, calculate the overlap with the ideal state and average over the initial states. In order to take into account relaxation processes, we consider the density matrix for the system composed of three states. We prepare an initial state:

$$\rho(-\infty) = |\psi(-\infty)\rangle\langle\psi(-\infty)| , \tag{34}$$

$$\psi(-\infty) = c_x(-\infty)|x\rangle + c_{\bar{x}}(-\infty)|\bar{x}\rangle \tag{35}$$

$$\text{with } \begin{pmatrix} c_x(-\infty) \\ c_{\bar{x}}(-\infty) \end{pmatrix} = \begin{pmatrix} \cos \theta_i/2 e^{-i\varphi_i/2} \\ \sin \theta_i/2 e^{i\varphi_i/2} \end{pmatrix} , \tag{36}$$

where θ_i and φ_i indicate the initial direction of the pseudospin. The time evolution of the density matrix is given by

$$\dot{\rho}(t) = -\frac{i}{\hbar} [H_0 + V, \rho] + \Gamma \rho , \tag{37}$$

where Γ includes the population relaxation and decoherence terms. After the time evolution we have the asymptotic state $\pi(\infty)$, which is actually $\pi(T_f)$ for a large enough time T_f , and calculate the fidelity defined by the overlap of the actual density matrix with the ideal density matrix which is obtained without any relaxation terms:

$$F = \langle \text{Tr}_{|x\rangle, |\bar{x}\rangle} \rho_{\text{ideal}}(\infty) \rho(\infty) \rangle_{c_x, c_{\bar{x}}} , \tag{38}$$

where the angular bracket means the average over the initial spin direction, namely:

$$\langle \dots \rangle_{c_x, c_{\hat{x}}} = \frac{1}{4\pi} \int_0^\pi d\theta_i \sin \theta_i \int_0^{2\pi} d\varphi_i \dots \quad (39)$$

Some numerical results will be presented for the fidelity and the residual population in the excited state $|T\rangle$. Because of the energy-time duality the following results can be applied for an arbitrary pulse width by scaling appropriately the off-resonance energy. But, for the definiteness, the optical pulse is assumed as $\text{sech}(t/t_p)$ with $t_p = 5\text{ps}$ and the time evolution is integrated over the time range of $-6t_p \leq t \leq 6t_p$. The relaxation parameters are chosen as

$$\hbar\Gamma_{T \rightarrow x} = \hbar\Gamma_{T \rightarrow \bar{x}} = 0.01\text{meV}, \quad \hbar\gamma_{T_x} = \hbar\gamma_{T_{\bar{x}}} = 0.05\text{meV}, \quad (40)$$

where $\Gamma(\gamma)$ indicates the population relaxation (decoherence) rate. The equations of motion for the density matrix elements are similar to those given from Eq. (58) to Eq. (64) in the later section. First of all, the rotation angle ϕ is plotted in Fig. 2 as a function of the off-resonance energy. The normalized off-resonance energy is defined by Δt_p , where Δ is given in Eq. (8), and is dimensionless. For the 2π pulse the rotation angle is monotonically increasing with increasing off-resonance. The fidelity of the spin rotation is exhibited in Fig. 3. The fidelity is improved with increasing off-resonance in general for the 2π and 4π pulses. For the 6π pulse, a strange behavior is seen. But it can be understood that a fidelity peak appears around the off-resonance energy where the rotation angle is almost 360 degrees, namely, the spin returns to the initial state and the deviation from the ideal time evolution is suppressed. Another important quantity is the residual population in the excited state $|T\rangle$ and is exhibited in Fig. 4. This is monotonically decreasing with increasing off-resonance.

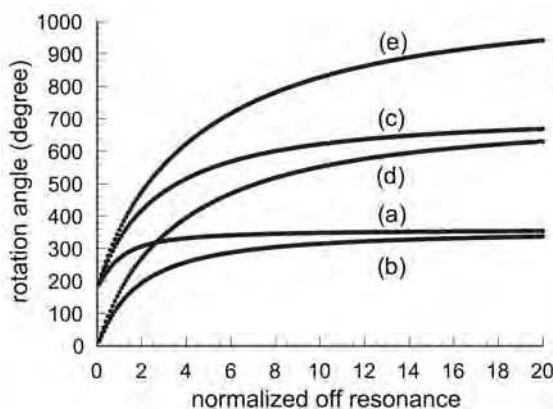


Fig. 2. Angles of the spin rotation are plotted as a function of the normalized off-resonance energy Δt_p for the pulse areas of (a) 2π , (b) 4π , (c) 6π , (d) 8π , and (e) 10π .

Analytically exact solutions are possible only for the sech pulses. In order to see the effect of the pulse shape, a Gaussian pulse is examined for the case of 2π pulse area. Results are exhibited in Figs. 5 and 6 and show that the sech pulse is better for the higher fidelity and the smaller population left in the excited state after the pulse.

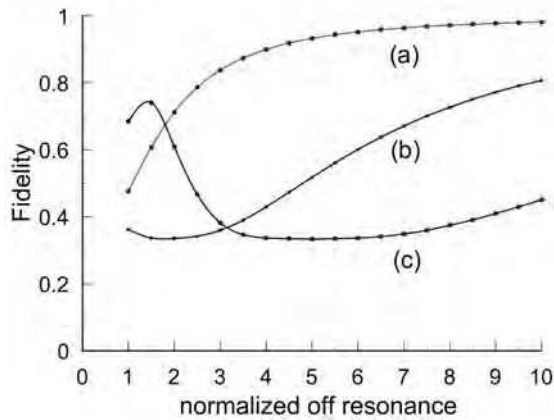


Fig. 3. Fidelity of the spin rotation of a single electron is plotted as a function of the normalized off-resonance. Curves (a), (b) and (c) correspond to the pulse area 2π , 4π and 6π , respectively.

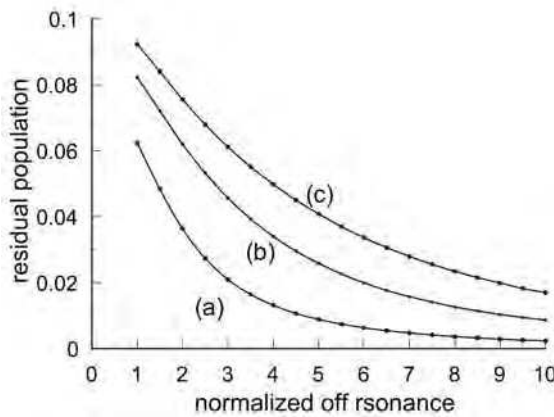


Fig. 4. Residual population in the excited state $|T\rangle$ after the spin rotation of a single electron is plotted as a function of the normalized off-resonance. Curves (a), (b) and (c) correspond to the pulse area 2π , 4π and 6π , respectively.

So far we have considered a typical Λ -type system composed of three energy levels. However, in the case of a singly charged semiconductor quantum dot, there are at least two excited states, namely the trion states, associated with two spin directions of the hole state. Thus, the four level system, as depicted in Fig. 7, is more appropriate. The fidelity of the spin rotation for the four level system is examined using the parameters:

$$\hbar\omega_T - \hbar\omega_{\bar{T}} = 0.05\text{meV} , \hbar\omega_{\bar{x}} - \hbar\omega_x = 0.05\text{meV} , \hbar\omega_x - \hbar\omega_y = 0.05\text{meV} , \tag{41}$$

$$\hbar\Gamma_{T \rightarrow x} = \hbar\Gamma_{T \rightarrow \bar{x}} = \hbar\Gamma_{\bar{T} \rightarrow x} = \hbar\Gamma_{\bar{T} \rightarrow \bar{x}} = 0.01\text{meV} , \tag{42}$$

$$\hbar\gamma_{T x} = \hbar\gamma_{T \bar{x}} = \hbar\gamma_{\bar{T} x} = \hbar\gamma_{\bar{T} \bar{x}} = 0.05\text{meV} , \tag{43}$$

where the Raman condition is applied to the left Λ -type transition. Results are given in Fig. 8 and show that the fidelity is not degraded by an additional Λ -type transition, especially for the 2π pulse area. Thus the spin rotation is expected to be robust against the overlap of several Λ -type transitions.

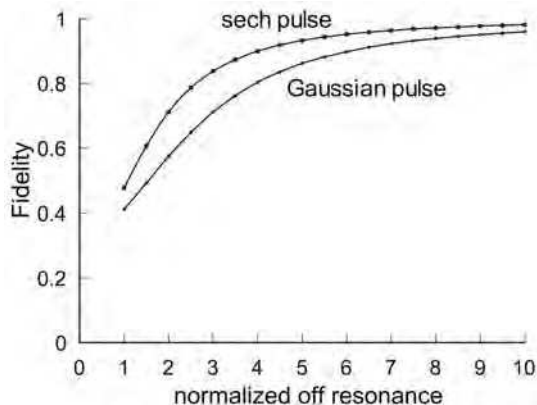


Fig. 5. Fidelity of the spin rotation of a single electron is compared between the cases of a Gaussian pulse and a sech pulse for the 2π pulse area.

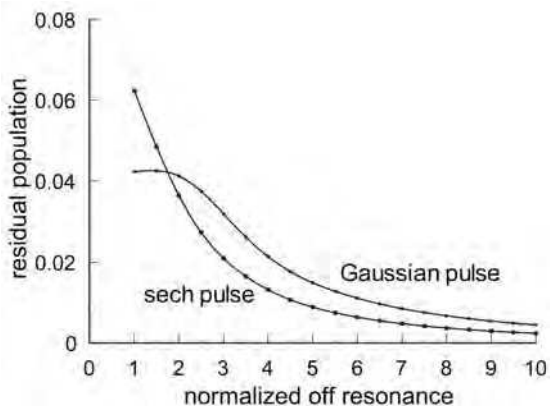


Fig. 6. Residual population in the excited state $|T\rangle$ after the spin rotation of a single electron is compared between the cases of a Gaussian pulse and a sech pulse for the 2π pulse area.

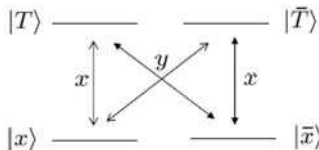


Fig. 7. Four level system composed of two electron spin states (lower levels) and two trion states with different hole spin states (upper levels). Allowed optical transitions are indicated by the x and y polarizations.

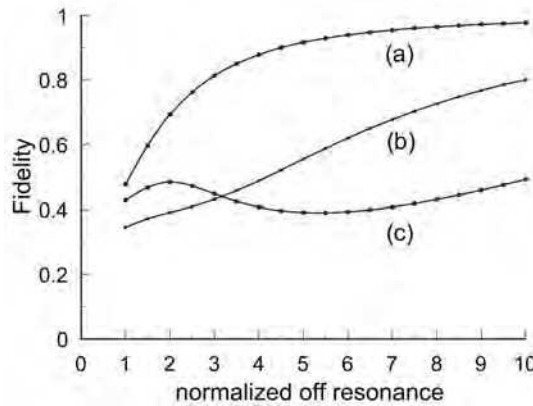


Fig. 8. Fidelity of the spin rotation of a single electron is plotted as a function of the normalized off-resonance in the four-level model. Curves (a), (b) and (c) correspond to the pulse area 2π , 4π and 6π , respectively.

3. Optical STIRAP method for spin rotation of two electrons

Now we extend the above arguments to the spin rotation of two electrons. This spin rotation is important because a qubit composed of the singlet state and one of the triplet states of two electrons confined in a semiconductor quantum dot was established and its electrical manipulation was demonstrated¹⁶. Here we examine the possibility of ultrafast spin rotation of two electrons by an optical means. As discussed above, the essential ingredient is the Λ -type transition with mutually orthogonal optical selection rules which enables the spin rotation of an arbitrary angle along an arbitrary direction. In the Faraday configuration the allowed optical transitions are exhibited in Fig. 9. The charged exciton state is depicted by X^{2-} . An additional superscript indicates the spin direction of the electron in the excited orbital state and an additional subscript represents the spin direction of the heavy hole in the lowest energy orbital state, namely,

$$|hh+\rangle = \left| \frac{3}{2} \frac{3}{2} \right\rangle, |hh-\rangle = \left| \frac{3}{2} - \frac{3}{2} \right\rangle, \tag{44}$$

where the left hand side indicates the missing state of the valence band electron in the state on the right hand side. There is a Λ -type transition but with the same optical selection rules. Thus the arbitrary spin rotation is not possible.

On the other hand, for the Voigt configuration in which a magnetic field is applied along the quantum dot plane (taken as the x axis), the optical selection rules are exhibited in Fig. 10 for the case associated with the light hole state. Here, an additional superscript attached to X^{2-} indicates the spin direction of the electron in the excited orbital state, namely, $+(-)$ for the $x(-x)$ direction and an additional subscript represents the spin direction of the light hole in the lowest energy orbital state, namely, $lh+$ or $lh-$ corresponding to

$$|lh+\rangle = \frac{1}{\sqrt{2}} \left(\left| \frac{3}{2} \frac{1}{2} \right\rangle + \left| \frac{3}{2} - \frac{1}{2} \right\rangle \right) \text{ or } |lh-\rangle = \frac{1}{\sqrt{2}} \left(-\left| \frac{3}{2} \frac{1}{2} \right\rangle + \left| \frac{3}{2} - \frac{1}{2} \right\rangle \right), \tag{45}$$

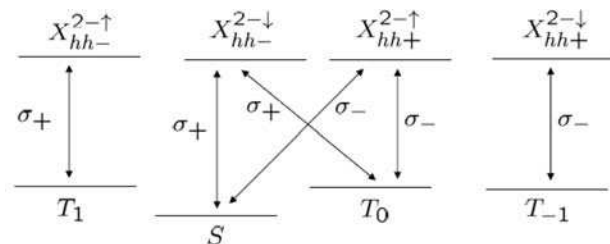


Fig. 9. Allowed optical transitions in the Faraday configuration for two electrons. The lower levels represent the four spin states of two electrons: the singlet (S) and three triplet (T_1 , T_0 , T_{-1}) states, whereas the upper levels exhibit the negatively doubly charged exciton states (X^{2-}) with indexes indicating the spin state of the electron in the excited orbital and the spin state of the heavy hole.

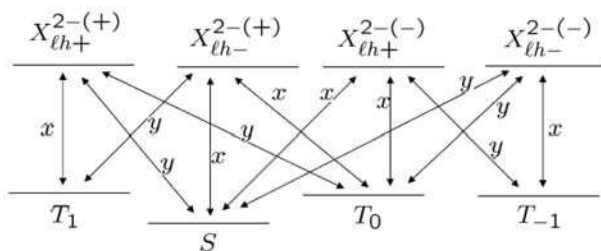


Fig. 10. Allowed optical transitions in the Voigt configuration for two electrons. The lower levels represent the four spin states of two electrons: the singlet (S) and three triplet (T_1 , T_0 , T_{-1}) states, whereas the upper levels exhibit the negatively doubly charged exciton states (X^{2-}) with indexes indicating the spin state of the electron in the excited orbital and the spin state of the light hole.

where the left hand side indicates the missing state of the valence band electron in the state on the right hand side. Then we find that the spin rotation by STIRAP is possible except for cases of the pseudospin composed of (S , T_0) and (T_1 , T_{-1}). The same situation holds also for transitions associated with the heavy hole. As seen in Fig. 10, the four levels in both the ground and excited states are energetically close to each other. In the excited states, they are lying within the range determined by the Zeeman energy difference, which is about several tens of μeV for 1 Tesla. In the ground states, the singlet state lies below the triplet states by the orbital excitation energy and the triplet states are close to each other within the Zeeman energy difference.

It is important to examine the fidelity of the spin rotation under the situation that several Λ -type transitions are overlapping within a similar energy range. As a model system we consider a five-level system as depicted in Fig. 11. Relative energy differences, population relaxation and decoherence rates employed are

$$\hbar\omega_1 - \hbar\omega_3 = 0.05\text{meV} , \hbar\omega_2 - \hbar\omega_0 = 0.05\text{meV} , \hbar\omega_4 - \hbar\omega_0 = 0.07\text{meV} , \quad (46)$$

$$\hbar\Gamma_{1\rightarrow 0} = \hbar\Gamma_{1\rightarrow 2} = \hbar\Gamma_{1\rightarrow 4} = \hbar\Gamma_{3\rightarrow 0} = \hbar\Gamma_{3\rightarrow 2} = \hbar\Gamma_{3\rightarrow 4} = 0.01\text{meV} , \quad (47)$$

$$\hbar\gamma_{10} = \hbar\gamma_{12} = \hbar\gamma_{14} = \hbar\gamma_{30} = \hbar\gamma_{32} = \hbar\gamma_{34} = 0.05\text{meV} . \quad (48)$$

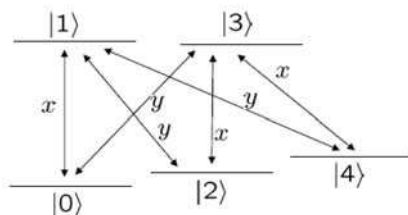


Fig. 11. Five level system composed of three lower levels and two upper levels. This is a simplest idealized model for studying the effect of overlapping Λ -type transitions.

Concerning the four levels composed of $|0\rangle$, $|1\rangle$, $|2\rangle$ and $|3\rangle$, the relevant parameters are the same as for the four-level system in Fig. 7. Thus, the effect of an additional level $|4\rangle$ can be examined. Results are exhibited in Fig. 12. An additional level degrades the coherence of the STIRAP process and reduces the fidelity of the spin rotation. However, in the case of 2π pulse area, the fidelity keeps a good value for large off-resonance energies.

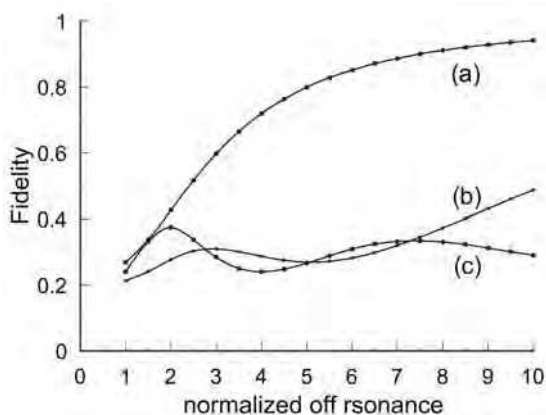


Fig. 12. Fidelity of the spin rotation of two electrons is plotted as a function of the normalized off-resonance in the five-level model. Curves (a), (b) and (c) correspond to the pulse area 2π , 4π and 6π , respectively.

Another important feature is the state initialization within the pseudospin subspace. When we want to rotate the pseudospin composed of $|0\rangle$ and $|2\rangle$ states in Fig. 11, the state should be initialized within this subspace. We examined the effect on the fidelity of the spin rotation of the incomplete state initialization. The fidelity is calculated for the case in which the state is prepared in the subspace spanned by the $|0\rangle$ and $|2\rangle$ states with the weight of 0.9 and in the $|4\rangle$ state with the weight of 0.1. Results are given in Fig. 13 with those for the complete initialization in which the state is prepared in the subspace spanned only by the $|0\rangle$ and $|2\rangle$ states. The fidelity loss proportional to the deviation from the perfect initialization is seen. Thus the state initialization should be carried out as perfect as possible. One possible way of the state initialization is the use of the singlet-triplet level crossing by the magnetic field tuning. At first we prepare the two electrons in the singlet state and then bring the system adiabatically to the crossing point. During the residence period at the crossing point,

the state mixing is induced by the spin-orbit interaction and the hyperfine interaction with nuclei, leading to an incoherent mixed state. This incoherent mixed state is sufficient to carry out the spin rotation. When the electron Zeeman energy is sufficiently large and three triplet states are well separated, the state initialization within the subspace composed of two crossing states such as (S, T_1) , (S, T_0) and (S, T_{-1}) will be established.

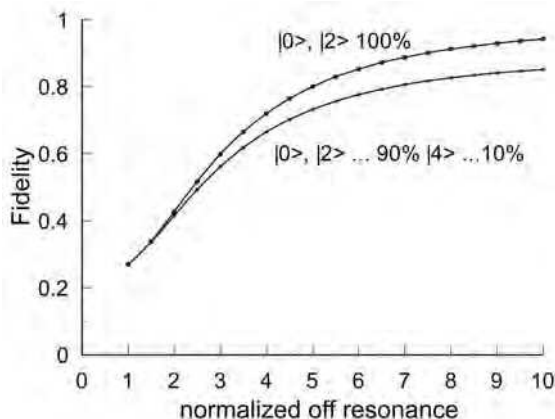


Fig. 13. Fidelity of the spin rotation of two electrons is plotted as a function of the normalized off-resonance in the five-level model for two cases, namely, one case where initially the population is prepared within the states $|0\rangle$ and $|2\rangle$ with 90% weight and in the state $|4\rangle$ with 10% weight and the other case where the population is prepared within the subspace spanned only by $|0\rangle$ and $|2\rangle$. The pulse area is 2π .

4. Spin state tomography of a single electron

The projective measurement of the spin state of a single electron is possible based on the Faraday/Kerr rotation of a linearly polarized light and this has been demonstrated experimentally very recently [42,43]. However, in the spin state tomography, all the components of the spin (s_x, s_y, s_z) , namely, the off-diagonal (coherence) components as well as the diagonal components of the density matrix should be measured. The density matrix of a single electron spin in the spin up and down bases is given by

$$\rho = \begin{pmatrix} \rho_{\uparrow\uparrow}^0 & \rho_{\uparrow\downarrow}^0 \\ \rho_{\downarrow\uparrow}^0 & \rho_{\downarrow\downarrow}^0 \end{pmatrix} = \frac{1}{2}(1 + \vec{s} \cdot \vec{\sigma}) \quad \text{with} \quad \vec{s} = (s_x, s_y, s_z), \quad (49)$$

$$s_x = \text{Tr} \rho \sigma_x = \rho_{\uparrow\downarrow}^0 + \rho_{\downarrow\uparrow}^0, \quad s_y = \text{Tr} \rho \sigma_y = -i(\rho_{\uparrow\downarrow}^0 - \rho_{\downarrow\uparrow}^0), \quad s_z = \text{Tr} \rho \sigma_z = \rho_{\uparrow\uparrow}^0 - \rho_{\downarrow\downarrow}^0, \quad (50)$$

where σ_i ($i = x, y, z$) is the Pauli spin matrix. The purity of this state is given by

$$\mathcal{P} = \text{Tr} \rho^2 = \frac{1}{2}(1 + (\vec{s})^2). \quad (51)$$

Thus, by measuring all the components (s_x, s_y, s_z) we can determine whether the state is a pure state or not.

In order to measure all the components (s_x, s_y, s_z) by an optical means, there should be at least one excited state which is connected to both the spin up and spin down states of the electron, in other words, there should be a Λ -type transition. This transition creates the coherence between the spin up and spin down states, rotates the spin and enables the spin state tomography. It is easily shown that such a Λ -type transition is not possible in the Faraday configuration. On the other hand, in the Voigt configuration in which an in-plane magnetic field is applied along, e.g., the x direction, the Λ -type transition is possible as depicted in Fig. 14 for the optical transitions associated with both the heavy hole and light hole bases. In Fig.14, the optical polarization selection rules are given in the x and y bases. The excited state is a trion state composed of a spin-singlet electron pair and a hole. The electron and hole states under an in-plane magnetic field are described by

$$|x+\rangle = \frac{1}{\sqrt{2}}(|\uparrow\rangle + |\downarrow\rangle), |x-\rangle = \frac{1}{\sqrt{2}}(-|\uparrow\rangle + |\downarrow\rangle), \tag{52}$$

$$|hh+\rangle = \frac{1}{\sqrt{2}}(|\frac{3}{2}\frac{3}{2}\rangle + |\frac{3}{2}-\frac{3}{2}\rangle), |hh-\rangle = \frac{1}{\sqrt{2}}(-|\frac{3}{2}\frac{3}{2}\rangle + |\frac{3}{2}-\frac{3}{2}\rangle), \tag{53}$$

$$|lh+\rangle = \frac{1}{\sqrt{2}}(|\frac{3}{2}\frac{1}{2}\rangle + |\frac{3}{2}-\frac{1}{2}\rangle), |lh-\rangle = \frac{1}{\sqrt{2}}(-|\frac{3}{2}\frac{1}{2}\rangle + |\frac{3}{2}-\frac{1}{2}\rangle), \tag{54}$$

where for the hole states the left hand side represents the missing state of the valence band electron in the state on the right hand side.

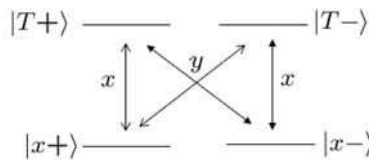


Fig. 14. Λ -type transitions for a single electron in the Voigt configuration. The lower levels indicate the two spin states of the electron, whereas the upper levels represent the trion states associated with the light hole or the heavy hole states. The polarization selection rules are given in terms of the x and y bases, where the in-plane magnetic field is applied in the x direction.

Now we discuss the scheme to measure the spin component of the electron. A probe light propagates along the z axis and its polarization rotation is measured in the transmission or reflection geometry. Thus the dielectric tensor represented in the bases of the electric field components in the x and y directions is relevant. In the theoretical analysis a single Λ -type transition will be considered with the level indexes as depicted in Fig. 15. An external test field is applied to estimate the dielectric tensor and is assumed as

$$\vec{\mathcal{E}}_{\text{test}}(t) = (\mathcal{E}_x \vec{e}_x + \mathcal{E}_y \vec{e}_y)e^{i\omega t} + \text{c.c.}, \tag{55}$$

where $\vec{e}_x(\vec{e}_y)$ is the unit vector in the $x(y)$ direction. The initial density matrix, which is to be fixed from the measurements, is given by

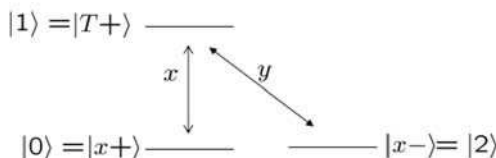


Fig. 15. A Λ -type transition is chosen from the left hand side of Fig. 14 and the levels are numbered to simplify theoretical expressions.

$$\rho(t = 0) = \begin{pmatrix} \rho_{00}^0 & \rho_{02}^0 & 0 \\ \rho_{20}^0 & \rho_{22}^0 & 0 \\ 0 & 0 & 0 \end{pmatrix}, \tag{56}$$

where the bases are chosen as $|0\rangle$, $|2\rangle$ and $|1\rangle$. The relevant equations of motion for the density matrix take the form:

$$\dot{\rho} = -\frac{i}{\hbar}[H_0 + V, \rho] + \Gamma\rho, \tag{57}$$

where H_0 and V are similar to those in Eqs. (2) and (3) and Γ includes the population relaxation and decoherence terms. Expressions for each matrix element are given below:

$$\dot{\rho}_{00} = i\Omega_x e^{i\omega t} \rho_{10} - i\Omega_x^* e^{-i\omega t} \rho_{01} + \Gamma_{1 \rightarrow 0} \rho_{11}, \tag{58}$$

$$\dot{\rho}_{11} = -i\Omega_x e^{i\omega t} \rho_{10} - i\Omega_y e^{i\omega t} \rho_{12} + \text{c.c.} - (\Gamma_{1 \rightarrow 0} + \Gamma_{1 \rightarrow 2}) \rho_{11}, \tag{59}$$

$$\rho_{22} = 1 - \rho_{00} - \rho_{11}, \tag{60}$$

$$\dot{\rho}_{01} = i\Omega_x e^{i\omega t} (\rho_{11} - \rho_{00}) - i\Omega_y e^{i\omega t} \rho_{02} + (i\omega_{10} - \gamma_{01}) \rho_{01}, \tag{61}$$

$$\dot{\rho}_{02} = i\Omega_x e^{i\omega t} \rho_{12} - i\Omega_y^* e^{-i\omega t} \rho_{01} + (i\omega_{20} - \gamma_{02}) \rho_{02}, \tag{62}$$

$$\dot{\rho}_{12} = i\Omega_x^* e^{-i\omega t} \rho_{02} + i\Omega_y e^{-i\omega t} (\rho_{22} - \rho_{11}) + (i\omega_{21} - \gamma_{12}) \rho_{12} \tag{63}$$

$$\text{with } \Omega_x = \frac{\mu_{01}^x \mathcal{E}_x}{\hbar}, \Omega_y = \frac{\mu_{21}^y \mathcal{E}_y}{\hbar}, \omega_{ij} = (E_i - E_j)/\hbar, \tag{64}$$

where μ_{ij}^k is the optical matrix element between the states $|\imath\rangle$ and $|\jmath\rangle$ for the light polarization in the k direction, E_i the energy of the state $|\imath\rangle$, $\Gamma_{i \rightarrow j}$ the population decay rate from the state $|\imath\rangle$ to the state $|\jmath\rangle$ and γ_{ij} is the decay rate of the coherence between the states $|\imath\rangle$ and $|\jmath\rangle$. In order to facilitate the analysis, the rapidly oscillating parts will be separated out as

$$\rho_{01}(t) = \bar{\rho}_{01}(t) e^{i\omega t}, \rho_{12}(t) = \bar{\rho}_{12}(t) e^{-i\omega t}, \tag{65}$$

where $\bar{\rho}_{01}$ and $\bar{\rho}_{12}$ are slowly varying amplitudes. ρ_{02} is also slowly varying because ω_{02} is very small compared with the optical transition energies. Then the equations of motion for these amplitudes become

$$\dot{\rho}_{01} = i\Omega_x(\rho_{11} - \rho_{00}) - i\Omega_y\rho_{02} + (i(\omega_{10} - \omega) - \gamma_{01})\bar{\rho}_{01} , \tag{66}$$

$$\dot{\rho}_{02} = i\Omega_x\bar{\rho}_{12} - i\Omega_y^*\bar{\rho}_{01} + (i\omega_{20} - \gamma_{02})\rho_{02} , \tag{67}$$

$$\dot{\bar{\rho}}_{12} = i\Omega_x^*\rho_{02} + i\Omega_y^*(\rho_{22} - \rho_{11}) + (i(\omega - \omega_{12}) - \gamma_{12})\bar{\rho}_{12} . \tag{68}$$

The stationary solutions within the linear response to the test field are given by

$$\rho_{01}^{st} = \frac{i\Omega_x\rho_{00}^0 + i\Omega_y\rho_{02}^0}{i\Delta - \gamma_{01}} , \rho_{21}^{st} = \frac{i\Omega_x\rho_{20}^0 + i\Omega_y\rho_{22}^0}{i(\Delta - \omega_{20}) - \gamma_{21}} \text{ with } \Delta = \omega_{10} - \omega . \tag{69}$$

Now the induced polarization and the corresponding susceptibility tensor χ are derived as

$$\vec{P} = \text{Tr } \vec{\mu}\rho^{st} = (\mu_{10}^x\rho_{01}^{st} + \mu_{12}^y\rho_{21}^{st})e^{i\omega t} + \text{c.c.} \tag{70}$$

$$\overset{\leftrightarrow}{\chi} \cdot \vec{\mathcal{E}} e^{i\omega t} + \text{c.c.} = \begin{pmatrix} \chi_{xx} & \chi_{xy} \\ \chi_{yx} & \chi_{yy} \end{pmatrix} \begin{pmatrix} \mathcal{E}_x \\ \mathcal{E}_y \end{pmatrix} e^{i\omega t} + \text{c.c.} \tag{71}$$

Assuming the large off-resonance: $\Delta \gg \omega_{20}, \gamma_{ij}$, we have

$$\overset{\leftrightarrow}{\chi}_A = A \begin{pmatrix} \rho_{00}^0 & i\rho_{02}^0 \\ -i\rho_{20}^0 & \rho_{22}^0 \end{pmatrix} \text{ with } A = \frac{|\mu_{01}^x|^2}{v_0\hbar\Delta} , \tag{72}$$

where v_0 is the normalization volume for the polarization density and the subscript A is attached for the later use. The dielectric tensor is given by

$$\overset{\leftrightarrow}{\epsilon} = \epsilon_0 + 4\pi \overset{\leftrightarrow}{\chi}_A , \tag{73}$$

where ϵ_0 is the background dielectric constant. In the case of large off-resonance, another Λ -type transition depicted in Fig. 16 should also be taken into account. After a similar calculation, the corresponding susceptibility $\overset{\leftrightarrow}{\chi}_B$ is estimated as

$$\overset{\leftrightarrow}{\chi}_B = B \begin{pmatrix} \rho_{22}^0 & i\rho_{20}^0 \\ -i\rho_{02}^0 & \rho_{00}^0 \end{pmatrix} \text{ with } B = \frac{|\mu_{21}^x|^2}{v_0\hbar\tilde{\Delta}} \text{ and } \tilde{\Delta} = \omega_{12} - \omega . \tag{74}$$

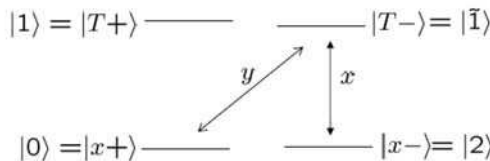


Fig. 16. A Λ -type transition is chosen from the right hand side of Fig. 14 and the levels are numbered to simplify theoretical expressions.

When the trion state associated with the heavy hole is considered, $\Delta \cong \tilde{\Delta}$ and hence $A \cong B$, because the g -factor of the heavy hole is very small. In the absence of the coupling between the heavy hole (hh) and the light hole (lh), the in-plane g -factor of the heavy hole is zero.

Actually, that g -factor is finite due to the hh-lh coupling. However, the g -factor of the heavy hole is one order of magnitude smaller than that of the light hole [25,44]. Then the total susceptibility becomes

$$\vec{\chi}_{\text{tot.}} = \vec{\chi}_A + \vec{\chi}_B \cong A \begin{pmatrix} 1 & i(\rho_{20}^0 + \rho_{02}^0) \\ -i(\rho_{20}^0 + \rho_{02}^0) & 1 \end{pmatrix}. \quad (75)$$

This indicates that only one component of the spin vector can be monitored. On the other hand, in the case of the light hole, the energy difference between $|1\rangle$ and $|\bar{1}\rangle$ is rather large and the contribution from either $\vec{\chi}_A$ or $\vec{\chi}_B$ is dominant. Then all the spin components can be measured as discussed below.

Now we discuss the measurement schemes to probe the spin components. For the moment, we consider the transmission geometry, assuming that the $\vec{\chi}_A$ is dominantly contributing to the dielectric tensor. Then the susceptibility tensor can be written in terms of s_x , s_y and s_z in Eq. (50) as

$$\vec{\chi}_A = \frac{A}{2} \begin{pmatrix} 1 + s_z & i s_x + s_y \\ -i s_x + s_y & 1 - s_z \end{pmatrix} \quad (76)$$

and the dielectric tensor is written as

$$\vec{\varepsilon} = \varepsilon_0 + 4\pi \vec{\chi}_A = (\varepsilon_0 + 2\pi A) \vec{1} + 4\pi \vec{\chi}'_A \quad (77)$$

$$\text{with } \vec{\chi}'_A = \frac{A}{2} \begin{pmatrix} s_z & i s_x + s_y \\ -i s_x + s_y & -s_z \end{pmatrix} = \frac{A}{2} [{}^t \vec{s} \cdot \vec{n} {}^t \vec{n} \cdot \vec{\sigma} + (\vec{\sigma} \times \vec{s}) \cdot \vec{n}], \quad (78)$$

where $\vec{n} {}^t \vec{n}$ is a dyadic form and the last expression is general for the axially symmetric case with the propagation vector \vec{n} of the probe light. Here $\vec{\chi}'_A$ is a Hermitian matrix and has eigenvectors associated with real eigenvalues χ_1 and χ_2 , namely

$$\vec{\chi}'_A \vec{u}_1 = \chi_1 \vec{u}_1, \quad \vec{\chi}'_A \vec{u}_2 = \chi_2 \vec{u}_2. \quad (79)$$

Then a probe light with an amplitude:

$$\vec{\mathcal{E}}_{\text{probe}}(t, z = 0) = (a \vec{u}_1 + b \vec{u}_2) e^{i\omega t} + \text{c.c.} = \vec{\mathcal{E}}_{\text{probe}}^{(+)} e^{i\omega t} + \text{c.c.} \quad (80)$$

propagates as

$$\vec{\mathcal{E}}_{\text{probe}}(t, z) = [a \vec{u}_1 e^{-ik_0 \sqrt{\varepsilon_1} z} + b \vec{u}_2 e^{-ik_0 \sqrt{\varepsilon_2} z}] e^{i\omega t} + \text{c.c.} \quad (81)$$

$$\text{with } k_0 = \frac{\omega}{c} \text{ and } \varepsilon_{1(2)} = \varepsilon_0 + 2\pi A + 4\pi \chi_{1(2)} = \tilde{\varepsilon}_0 + 4\pi \chi_{1(2)}. \quad (82)$$

For a thin sample, e.g., a single quantum dot layer, $k_0 z \ll 1$ and the phase factor can be expanded with respect to this smallness parameter. Then the transmitted field is obtained as

Thank You for previewing this eBook

You can read the full version of this eBook in different formats:

- HTML (Free /Available to everyone)
- PDF / TXT (Available to V.I.P. members. Free Standard members can access up to 5 PDF/TXT eBooks per month each month)
- Epub & Mobipocket (Exclusive to V.I.P. members)

To download this full book, simply select the format you desire below

